METHODS FOR GENERATING MULTIZONE FIELDS WITH LOW RISK OF INTERFERENCE

Mark Poletti

Callaghan Innovation, PO Box 31-310, Lower Hutt, New Zealand
email: mark.poletti@callaghaninnovation.govt.nz

Multizone sound fields allow multiple listeners, seated at different positions within a single sound reproduction system, to hear independent audio events. One of the limitations is that interference can occur between zones, particularly when the direction of sound propagation in one zone is in line with another zone. One solution to this problem is to restrict the direction of sound propagation to avoid the issue. If the loss of directional control is acceptable, then the sound field can be divided into strips within which independent sound fields can be created with low risk of interference. This paper considers two approaches to generating such sound fields in the 2D case. In the first, invariant 2D Bessel beams are derived, which produce unidirectional fields that do not disperse. The second approach uses a mode-weighting approach to produce more localised beams without side lobes. The relative effectiveness of the two approaches is investigated through numerical simulations.

Keywords: Multizone, surround sound, personal sound

1. Introduction

Personal sound systems aim to provide independent audio streams for multiple listeners [1], [2]. To achieve this using a single sound reproduction system requires that multiple reproduction zones be established with independent sound fields in each [3]–[5]. One approach is to maximise the acoustic contrast between zones [6]–[9]. The approach can be extended using intensity control to include control of direction [10]. An alternative approach is to maximise the energy difference between two zones [11]. More generally, a trade-off can be made between the requirement of maximum contrast and the desire for directional control [12].

Multi-zone reproduction is relatively easy to achieve when the direction of sound propagation within a zone is not in line with another zone, but when sound in one zone propagates towards another zone, it must diffract around the other zone to avoid interference. This is achievable at low frequencies [13] but at high frequencies it is more difficult [14]. Multizone fields can also be generated using the formalism of Wave Field Synthesis [15].

An alternative approach to avoid interference is to produce a sound field with a single direction of propagation, as occurs in personal sound systems using a planar array [6], [7], [15]. While these 1D multizone fields provide no directional control, they allow the size of the zone in the direction of propagation to be extended, particular when using circular or spherical arrays which can produce less dispersive beams than planar arrays. For example, in the case of two zones, a reproduction system can produce two half-space fields, each occupying half of the reproduction area [16].

This paper discusses the generation of 1D multizone fields using circular arrays. Two approaches are described. In the first, invariant Bessel beams are derived. In the second, modal bandpass windowing the coefficients of a plane wave field produce beams of sound propagating in the same direction. The work is restricted to the 2D case for simplicity. The performance of the two approaches is quantified via numerical simulations.

2. Theory

2.1 2D Invariant beams

A general solution to the 2D wave equation in polar coordinates has the Herglotz form

$$p(R,\phi)=\frac{1}{2\pi}\int_{-\pi}^{\pi}A(\phi_i)e^{ikR\cos(\phi-\phi_i)}d\phi_i\ , \tag{1}$$

where $x=R\cos\phi$, $y=R\sin\phi$ and $A(\phi_i)$ is the 2D angular spectrum. Writing $A(\phi_i)$ in the form

$$A(\phi_i)=\sum_{m=-\infty}^{\infty}\alpha_m e^{im\phi_i} \tag{2}$$

and substituting the Jacobi-Anger expansion of the plane wave term,

$$e^{ikR\cos\phi}=\sum_{m=-\infty}^{\infty}i^m J_m(kR)e^{im\phi}\ , \tag{3}$$

yields the well-known plane wave expansion

$$p(R,\phi)=\sum_{m=-\infty}^{\infty}\alpha_m i^m J_m(kR)e^{im\phi}\ . \tag{4}$$

In Cartesian coordinates the field (1) has the form

$$p(x,y)=\frac{1}{2\pi}\int_{-\pi}^{\pi}A(\phi_i)e^{ik(x\cos\phi_i+y\sin\phi_i)}d\phi_i\ . \tag{5}$$

Using the Bessel expansion (3) for the cosine factor and

$$e^{iky\sin\phi_i}=\sum_{m=-\infty}^{\infty}J_m(ky)e^{im\phi_i} \tag{6}$$

for the sine factor yields the Cartesian expansion

$$p(x,y)=\sum_{n=-\infty}^{\infty}\sum_{m=-\infty}^{\infty}\alpha_n i^{n+m}J_{n+m}(kx)J_m(ky)\ . \tag{7}$$

An invariant beam may be generated by a sum of plane waves arriving from a limited range of directions $\phi_i\in[-\phi_0,\phi_0]$ from the *x*-axis [17]. If ϕ_0 is sufficiently small then $\cos\phi_i\approx 1$ and (5) can be approximated as

$$\tilde{p}(x,y)=e^{ikx}\frac{1}{2\pi}\int_{-\pi}^{\pi}A(\phi_i)e^{iky\sin\phi_i}d\phi_i\ . \tag{8}$$

Substituting the expansions for the two terms in the integral from (2) and (6) yields the equivalent invariant approximations

$$\tilde{p}(x,y)=e^{ikx}\sum_{m=-\infty}^{\infty}\alpha_m(-1)^m J_m(ky)=e^{ikx}\sum_{m=-\infty}^{\infty}\alpha_m J_m(-ky)=e^{ikx}\sum_{m=-\infty}^{\infty}\alpha_{-m}J_m(ky)\ . \tag{9}$$

These approximate the exact expansion in (7). Comparing (7) and (9), it is apparent that

$$\sum_{n=-\infty}^{\infty}i^{n-m}\alpha_n J_{n-m}(kx)\approx e^{ikx}\alpha_m\ . \tag{10}$$

This identity holds provided that the coefficients α_m are consistent with a narrow range of angles. It can be further validated as follows. Since the LHS of (10) is the convolution of α_m and $i^m J_m(kx)$ it can be written

$$\left[i^m J_m(kx)\right]*\alpha_m\approx e^{ikx}\alpha_m\ . \tag{11}$$

The discrete Fourier transform of each side is

$$e^{ikx\cos\phi_i}A(\phi_i)\approx e^{ikx}A(\phi_i), \tag{12}$$

which is the invariant approximation.

Consider, now, the coefficients

$$\alpha_m = J_q\left(m\phi_0\right). \tag{13}$$

From (2), these produce an angular spectrum of the form [18], (11.4.24)

$$A(\phi_i)=\begin{cases}\dfrac{2i^q}{\phi_0}\dfrac{T_q\left(\phi_i/\phi_0\right)}{\sqrt{1-\left(\phi_i/\phi_0\right)^2}}, |\phi_i|<\phi_0\\ 0, \quad |\phi_i|>\phi_0\end{cases}, \tag{14}$$

where $T_q(.)$ is the qth order Chebyshev function. For small ϕ_0 this will produce an approximately invariant beam. Substituting (13) in the first form of the invariant approximation in (9), and using the Bessel summation approximation (Appendix A)

$$\sum_{m=-\infty}^{\infty}(-1)^m J_q\left(m\phi_0\right)J_m\left(ky\right)\approx(-1)^q J_m\left(ky\sin\phi_0\right) \tag{15}$$

yields the invariant approximation

$$\tilde{p}(x,y)=(-1)^q e^{ikx}J_q\left(ky\sin\phi_0\right), \tag{16}$$

which is a 2D cylindrical Bessel beam [19],[20]. Hence, cylindrical sound field coefficients defined in terms of a Bessel function (13) produce a 2D cylindrical Bessel beam. The Bessel beam produces nulls at $y=y_{\text{null}}$ where

$$ky_{null}\sin\phi_0 = z_{q,v}, \tag{17}$$

where $z_{q,v}$ is the vth zero of the qth Bessel function.

Fig. 1a shows the real part of the exact sound field generated from (4) for a frequency of f_0 = 1 kHz and an angle $\phi_0 = 10$ degrees. The invariant approximation from (16) is shown in Fig. 1b. The main differences between the two fields are that the behaviour of the actual field in the null regions differs and, since the angular spectrum (14) has peaks at $\phi_i = \pm\phi_0$, the variation in x is better approximated as $\exp\left(ikx\cos\phi_0\right)$ than $\exp\left(ikx\right)$ as shown in (16).

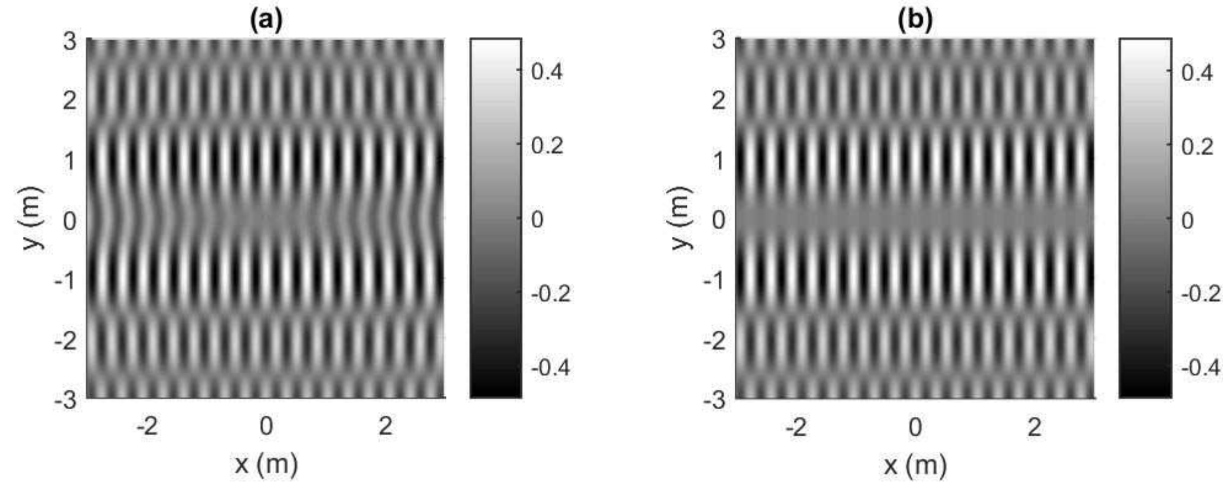

Figure 1: Field (a) and theoretical Bessel beam (b), q=2, ϕ_0 = 10 degrees, f_0 = 1 kHz,

2.2 Modal bandpass beams

It has been shown that a half space field of a plane wave can be generated if the amplitudes of the negative order modes are suppressed [16]. It was also shown that the half-space boundary can be shifted a distance $-y_0$ along the y-axis by shifting the mode weighting by a positive offset of approximately $m_0 = ky_0$. More generally, an approximately invariant beam can be generated at center y_0 with two-sided width $2y_d$ by bandpass weighting the mode amplitudes of a plane wave with a window of width $2m_d + 1$ where

$$m_d = [ky_d] \tag{18}$$

and [.] denotes rounding to the nearest integer. Furthermore the beam can be shifted by y_0 using a mode offset

$$m_0 = -[ky_0]. \tag{19}$$

The suppression of the field outside its intended width can be improved by using a smooth windowing of the mode coefficients [16]. Here, a two-sided window with raised cosine roll-off at each end will be used. The roll-off is governed by specifying the percentage of the window that has values of one. Raised cosine roll-offs are then applied at each end. The window is shown in Figure 2a for a beam width of 1m, shifted to y = 1m, with a frequency of 1 kHz and 25% flatness. The corresponding sound field is shown in Figure 2b. The beam width is reduced by the roll-off of the mode weighting, and is largely confined within the desired range of 0 to 2 m. The beam magnitude tends to fan out slightly from the $x = 0$ line and so is not as invariant as the beams described in section 2.1.

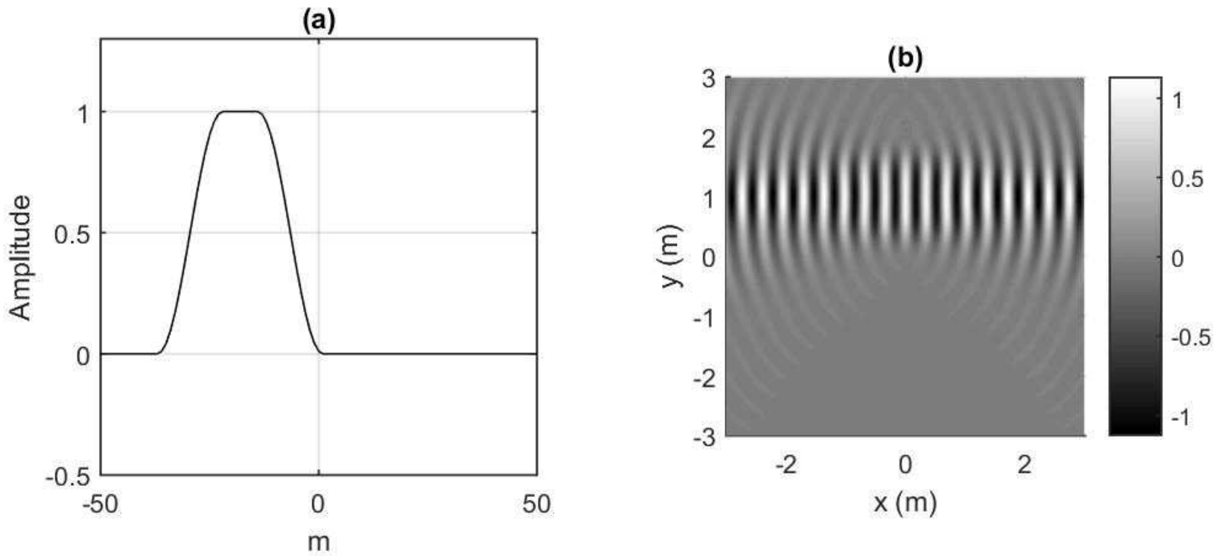

Figure 2: Modal bandpass beam spectrum (a) and field (b), f_0 = 1 kHz

3. Simulations

The two approaches to generating invariant beams described above can be applied to producing 1D multizone fields. The beam widths must also be frequency-invariant. Using Bessel beams, a two-zone field can be generated using beams offset by $y = \pm y_0$ so that the first null of one beam is positioned at the peak of the other. The corresponding mode index offset is $m_0 = \pm[ky_0]$. To maintain a frequency-invariant beam the angle ϕ_0 is varied with frequency, from (17), as

$$\phi_0 = \begin{cases} \sin^{-1}\left(\dfrac{z_{0,1}}{2ky_0}\right), \; ky_0 \geq z_{0,1} \\ \pi/2, \;\; ky_0 < z_{0,1} \end{cases}. \tag{20}$$

With a finite head radius R_h, a listener at the peak of one beam will not be able to experience complete suppression of the other beam. The relative amplitude of the unwanted Bessel beam compared to that of the desired beam is given by

$$\gamma = \frac{J_0\left(z_{1,0} + z_{1,0}R_h/2y_0\right)}{J_0\left(z_{1,0}R_h/2y_0\right)}. \tag{21}$$

For example, with R_h = 90 mm and y_0 = 1 m, $\gamma = -25$ dB which is a reasonable level of attenuation.

Using the bandpass windowed mode approach, any number of beams can be produced with arbitrary widths. Here, a three-zone example will be given, with beams positioned at y = –1, 0 and 1 m, with beam widths of 1m (y_d = 0.5 m).

Simulations were written in Matlab using a circular array of L = 351 2D sources at a radius of 2m, producing a spatial aliasing frequency of 4.7 kHz. A sample frequency of 8 kHz was used to avoid aliasing throughout the reproduction area [13]. The source weightings were derived as [13]

$$w_l = \frac{1}{L}\sum_{m=-M}^{M} i^m \frac{\alpha_m}{H_m\left(kR_L\right)} e^{im\phi_l}. \tag{22}$$

An FFT size of 200 points was used and the weights were determined at 100 positive frequencies and the sound field produced at the time when the resulting broadband pulse was positioned at x = 1m and x = 0, to show how the pulse shape and localisation of the beam varied with position.

3.1 Results

Two Bessel beam pulses were generated at y = –1 and y = 1 m. The fields are shown when the pulses are at x = 1, in Fig. 3, and when they are at x = 0, in Fig. 4. The Bessel beams maintain their shape as the pulse propagates across the array.

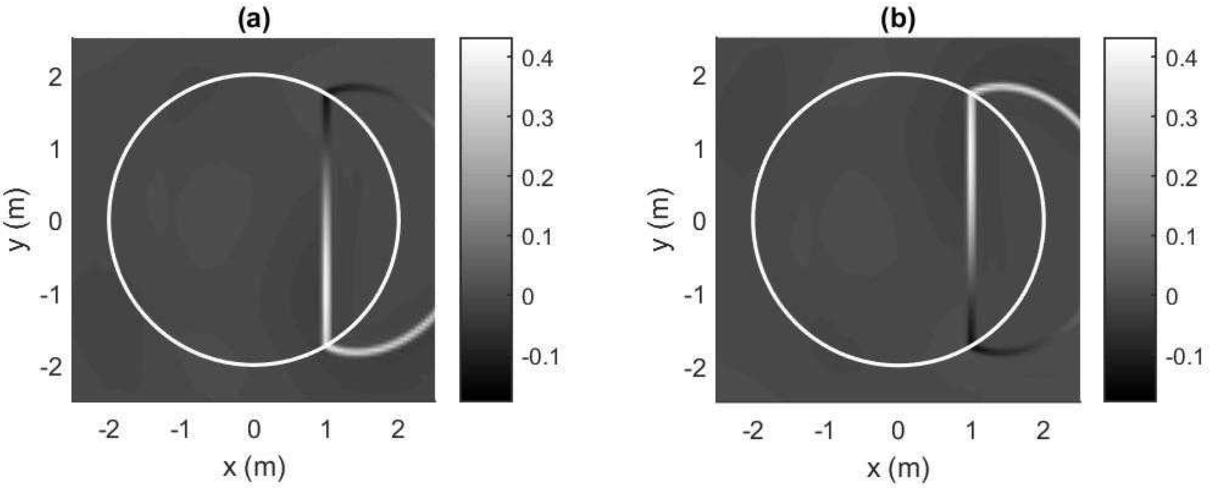

Figure 3: Bessel beams at y = –1 (a) and y = 1 (b), for x = 1m

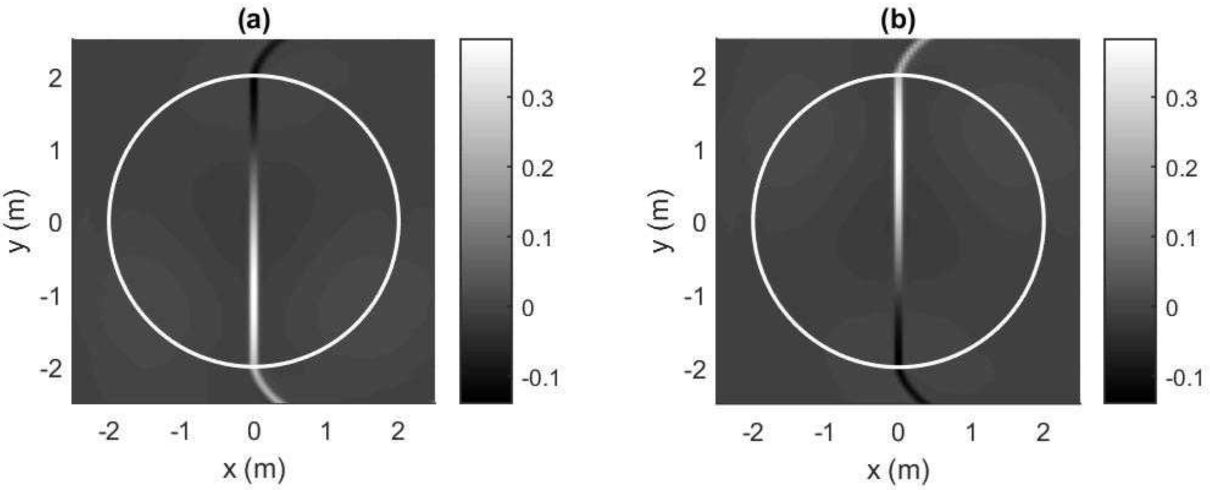

Figure 4: Bessel beams at y = –1 (a) and y = 1 (b), for x = 0m

The fields produced using three modal bandpass beams are shown in Figures 5 and 6. The pulses do not maintain their shape to the same extent as the invariant Bessel beams, but are well separated at the center of the reproduction region.

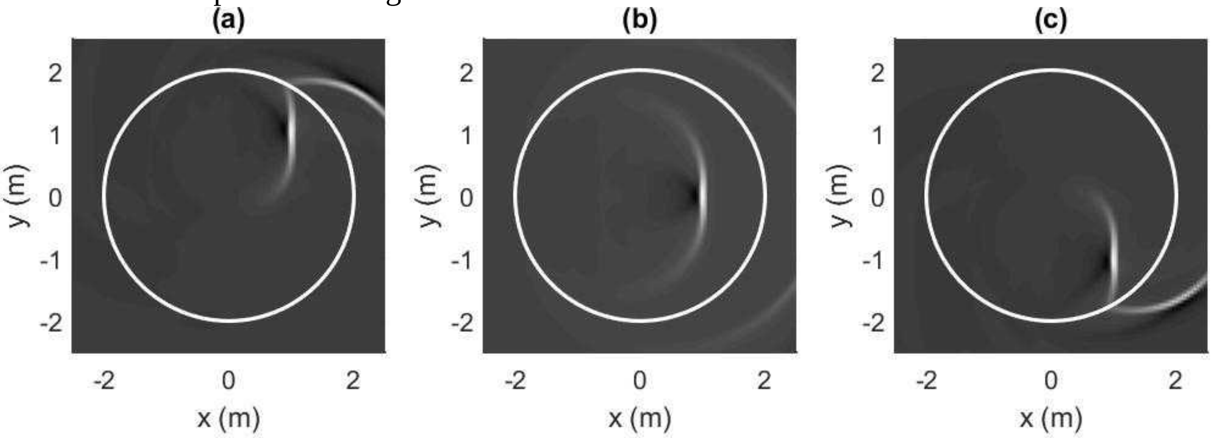

Figure 5: Modal bandpass beams at y = –1 (a), y = 0 (b) and y = 1 (c), at x = 1m

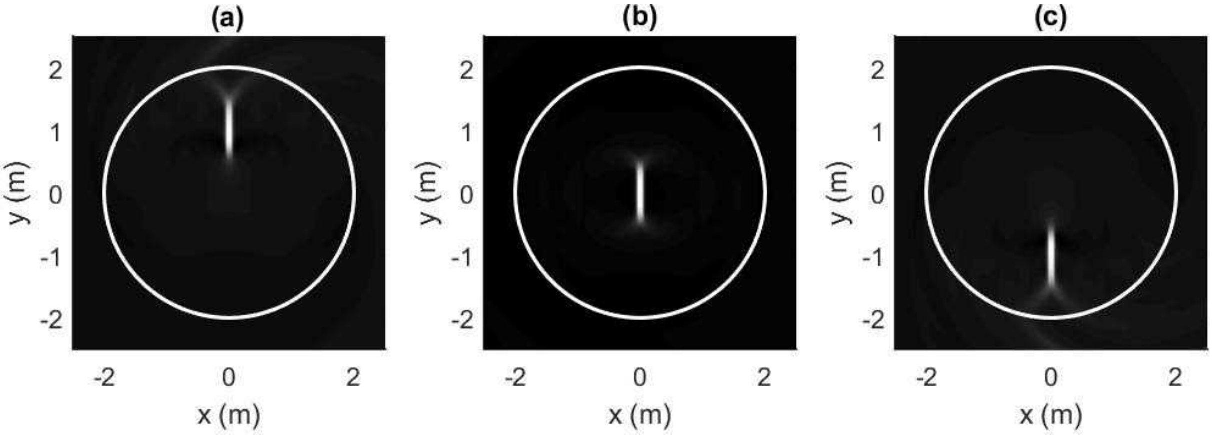

Figure 6: Modal bandpass beams at y = –1 (a), y = 0 (b) and y = 1 (c), at x = 0m

4. Conclusions

This paper has investigated the generation of sound beams which can create localised sound fields within a single array, for a single direction of arrival. Such 1D multizone fields may be of use where directionality is not critical, but the sound must be produced over a wider zone for several listeners. A family of 2D Bessel beams has been derived which remain relatively invariant, and which are well-suited to the 1D multizone problem. However, the suppression of each beam at the center of the other is relatively poor because the field is zero only along a line. One solution to this would be to position a zeroth order and a higher-order Bessel pulse at y=0. The higher order pulse would produce a broader zero around y=0. The zeroth order beam would be arranged so that its first zero coincided with the peak of the higher-order beam. This approach has been investigated but the results are not reported here. An interesting theoretical aspect of this work is that 2D cylindrical Bessel beams are formed by a 2D integral over a narrow range of angles of incidence, which is equivalent to the generation of 3D spherical Bessel beams discussed in [17].

The modal bandpass beams allow an arbitrary number of beams to be generated with any width and so are more flexible than the Bessel beams. However, being non-invariant, they tend to disperse both before and after they cross the center of the array. Therefore the suppression of the unwanted beams will be less effective at these positions.

5. Appendix A

Consider the following Bessel summation

$$g(x,\phi_0)=\sum_{m=-\infty}^{\infty} f(m\phi_0)J_m(x), \tag{A 1}$$

where $f(.)$ is an arbitrary continuous bandlimited function. We show that, for small angles ϕ_0,

$$g(x,\phi_0)\approx f(x\sin\phi_0). \tag{A 2}$$

An arbitrary bandlimited function can be written

$$f(x)=\frac{1}{2\pi}\int_{-B}^{B} F(\omega)e^{i\omega x}d\omega. \tag{A 3}$$

Substituting in (A 1) yields

$$g(x,\phi_0)=\frac{1}{2\pi}\int_{-B}^{B} F(\omega)\sum_m e^{i\omega m\phi}J_m(x)d\omega=\frac{1}{2\pi}\int_{-B}^{B} F(\omega)e^{ix\sin(\omega\phi_0)}d\omega. \tag{A 4}$$

For small $\omega\phi_0$ this is approximately

$$g(x,\phi_0)\approx\frac{1}{2\pi}\int_{-B}^{B} F(\omega)e^{ix\sin(\phi_0)\omega}d\omega= f(x\sin\phi_0). \tag{A 5}$$

The approximation is good for small angles and for functions that have small bandwidths so that ω is also restricted in range. Hence, for small ϕ_0,

$$\sum_{m=-\infty}^{\infty} f(m\phi_0)J_m(x)\approx f(x\sin\phi_0). \tag{A 6}$$

The normalised error in the approximation may be defined as

$$\varepsilon=\frac{\left(g(x,\phi_0)-f(x\sin\phi_0)\right)^2}{\max_x\left\{\left(f(x\sin\phi_0)\right)^2\right\}}. \tag{A 7}$$

This error is shown in Figures A.1 for $f(x)=J_q(x)$ for *q* = 0 to 3 and for $\phi_0=10$ degrees. The error is below –40 dB for all values of *x*.

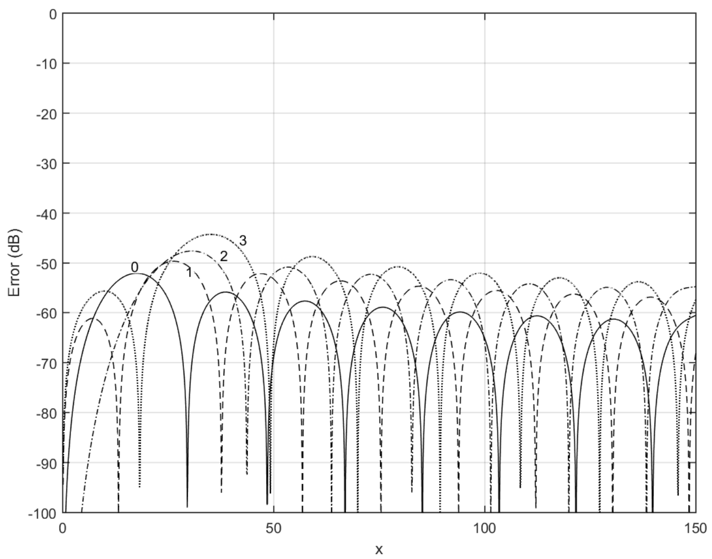

Figure A 1: Expansion error

REFERENCES

[1] W. F. Druyvesteyn and J. Garas, "Personal Sound," *J. Audio Eng. Soc.*, vol. 45, no. 9, pp. 685–701, 1997.

[2] T. Betlehem, W. Zhang, M. A. Poletti, and T. D. Abhayapala, "Personal sound zones," *IEEE Signal Proc. Mag.*, vol. 32, no. 2, pp. 81–91, Mar. 2015.

[3] M. A. Poletti, "An Investigation of 2D Multizone Surround Sound Systems," in *AES 125th Convention*, 2008.

[4] P. Coleman, P. J. B. Jackson, M. Olik, M. Møller, M. Olsen, and J. Abildgaard Pedersen, "Acoustic contrast, planarity and robustness of sound zone methods using a circular loudspeaker array," *J. Acoust. Soc. Am.*, vol. 135, no. 4, pp. 1929–1940, 2014.

[5] Y. J. Wu and T. D. Abhayapala, "Spatial Multizone Soundfield Reproduction: Theory and Design," *IEEE Trans. Audio, Speech Lang. Proc.*, vol. 19, no. 6, pp. 1711–1720, 2011.

[6] J.-W. Choi and Y.-H. Kim, "Generation of an acoustically bright zone with an illuminated region using multiple sources," *J. Acoust. Soc. Am.*, vol. 111, no. 4, pp. 1695–1700, 2002.

[7] J.-Y. Park, J.-H. Chang, and Y.-H. Kim, "Generation of independent bright zones for a two-channel private audio system," *J. Audio Eng. Soc.*, vol. 58, no. 5, pp. 382–393, 2010.

[8] J. Chang, C.-H. Lee, J.-Y. Park, and Y.-H. Kim, "A realization of sound focused personal audio system using acoustic contrast control," *J. Acoust. Soc. Am.*, vol. 125, no. 4, pp. 2091–2097, 2009.

[9] J.-H. Chang, J.-Y. Park, and Y.-H. Kim, "Scattering effect on the sound focused personal audio system," *J. Acoust. Soc. Am.*, vol. 125, no. 5, pp. 3060–3066, 2009.

[10] J.-W. Choi and Y.-H. Kim, "Manipulation of sound intensity within a selected region using multiple sources," *J. Acoust. Soc. Am.*, vol. 116, no. 2, pp. 843–852, 2004.

[11] M. Shin, S. Q. Lee, F. M. Fazi, P. A. Nelson, D. Kim, S. Wang, K. H. Park, and J. Seo, "Maximization of acoustic energy difference between two spaces," *J. Acoust. Soc. Am.*, vol. 128, no. 1, pp. 121–131, 2010.

[12] P. Coleman, P. Jackson, M. Olik, and J. A. Pedersen, "Optimizing the planarity of sound zones," in *AES 52nd Intl. Conf.*, 2013.

[13] M. A. Poletti and F. M. Fazi, "An approach to generating two zones of silence with application to personal sound systems," *J. Acoust. Soc. Am.*, vol. 137, no. 2, pp. 598–605, 2015.

[14] Y. J. Wu and T. D. Abhayapala, "Multizone 2D soundfield reproduction via spatial band stop filters," in *IEEE Workshop on Applications of Signal Processing to Audio and Acoustics*, 2009.

[15] K. Helwani, S. Spors, and H. Buchner, "The synthesis of sound figures," *Multidim. Syst. Sign. Process.*, vol. 25, pp. 379–403, 2014.

[16] M. A. Poletti and F. M. Fazi, "Generation of half-space sound fields with application to personal sound systems," *J. Acoust. Soc. Am.*, vol. 139, no. 3, pp. 1294–1302, 2016.

[17] M. A. Poletti, "Spherical coordinate descriptions of cylindrical and spherical Bessel beams," *J. Acoust. Soc. Am.*, *Submitt.*

[18] M. Abramowitz and I. A. Stegun, *Handbook of mathematical functions with formulas, graphs and mathematical tables*. National Bureau of Standards, 1972.

[19] J. Durnin, J. Miceli, and J. H. Eberly, "Diffraction-free beams," *Phys. Rev. Lett.*, vol. 58, no. 15, pp. 1499–1501, 1987.

[20] D. McGloin and K. Dholakia, "Bessel beams: Diffraction in a new light," *Contemp. Phys.*, vol. 46, no. 1, pp. 15–28, 2005.